WAVELET-BASED FUSION OF SPOT/VEGETATION AND ENVISAT/ ASAR WIDE SWATH DATA FOR WETLAND MAPPING

Toon Westra, Koen C. Mertens and Robert R. De Wulf

Ghent University, Department of Forest and Water Management, Coupure Links 653, 9000 Ghent, Belgium,
Toon.Westra@UGent.be, Koen.Mertens@UGent.be, Robert.Dewulf@UGent.be

ABSTRACT

SPOT/VEGETATION D-10 and ENVISAT/Advanced Synthetic Aperture Radar (ASAR) Wide Swath data are combined using a wavelet-based fusion technique. The objectives of the fusion are feature enhancement and improvement of classification accuracy of a wetland area, located in the Lake Chad basin. The fusion results are compared to those obtained by the intensity hue saturation (IHS) method and the principal component (PC) method. Evaluation is performed by visual inspection and by analyzing the classification results using a maximum likelihood classifier.
The results show that the fusion methods based on the wavelet transform outperform the IHS and PC methods for both objectives (feature enhancement and classification accuracy). The wavelet-based methods better preserve spectral contents, while spatial details remain apparent. Classification of the wavelet-based fused images yields significantly higher accuracies.

1 INTRODUCTION

The wetlands located in the Lake Chad basin are both ecologically and economically of exceptional importance. Therefore, mapping and monitoring these ecosystems is a very important task. Due to the extent and inaccessibility of these wetlands, the only feasible way to achieve this, is by means of remote sensing.
In this study, both ENVISAT/Advanced Synthetic Aperture Radar (ASAR) Wide Swath data and SPOT/VEGETATION (VGT) D-10 data are used. ASAR data acquisition is weather independent, which is an advantage in tropical regions, where cloud cover is often present. On ASAR images wetland vegetation often shows high radar backscatter values, due to (1) double bounce interaction of the microwave radiation with emergent vegetation and the water surface and (2) higher moisture content of the vegetation. Hence flooded vegetation can easily be separated from dry land vegetation. However, not all land cover classes can be as easily detected using ASAR data. Therefore optical data is used as well, providing complementary information and facilitating the image interpretation process. The benefits of combining SAR and optical data for studying wetlands have been illustrated by several authors [1], [2].
Image fusion techniques make it possible to combine data with different characteristics. According to Pohl and Van Genderen [3], image fusion is the combination of two or more images to create a new image containing more information by using a certain algorithm. It can be performed at three different processing levels: pixel, feature and decision level. In this study, a pixel level approach is followed. A fusion technique based on the discrete two-dimensional wavelet transform is used and compared to fusion methods based on intensity hue saturation (IHS) transformation and principal component (PC) transformation. The main objectives of the image fusion are feature enhancement and improved classification accuracy. Therefore quality of the fused images is evaluated (1) by visual inspection of a color composite image of the fused bands, and (2) by quantitatively comparing the classification results based on the fused images, using a parametric classifier.
In remote sensing, wavelet-based fusion methods have primarily been used to combine panchromatic and multi-spectral data, in order to improve spatial resolution and preserve multi-spectral information [4]-[7]. In [8], a wavelet-based method is used to fuse RADARSAT-1/ ScanSAR data with NOAA/ AVHRR data for feature enhancement.

2 STUDY AREA

The Logone floodplain, located in the Lake Chad basin, stretches from Nigeria across northern Cameroon to Chad, approximately between 10°50'N and 12°30'N, and between 14°0'E and 15°20'E (Fig. 1). The floodplain measures about 200 km from north to south and its width is 40 km.
Flooding of the plain starts with the onset of the rainy season in early July. In September, the Logone River rises and the entire plain is flooded with up to several meters of water. In November, the flood starts receding and by the end of February, the plain is entirely dry again.

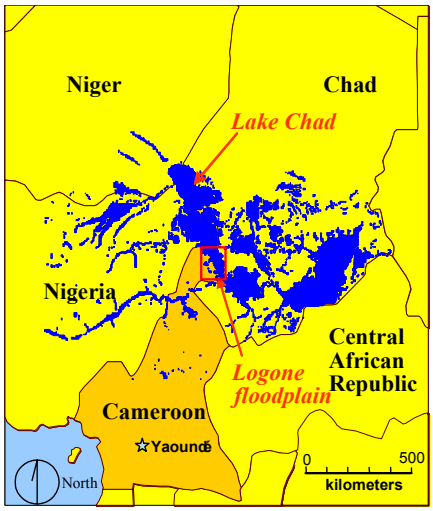

Fig. 1. Study area

The wetland vegetation consists mainly of different species of grasses that have adapted to varying degrees of inundation. The natural dry land vegetation consists of woodland savanna, but is now largely replaced by small-scale agriculture and grassy areas with thorny shrubs.

3 IMAGE FUSION

The image fusion technique considered in this study is based on the multiresolution wavelet decomposition [9]. The wavelet decomposition of an image results in a set of approximation images, representing the original scene at a lower scale or resolution, and a set of detail images, containing information about the details that exist between two successive resolution levels. Implementation of the wavelet decomposition can be done using different algorithms: the discrete wavelet transform [10] and the 'à trous' algorithm [11]. In the proposed method, the *à trous* algorithm is applied.
The fusion results of the proposed methods are compared to those obtained using established fusion methods: the IHS method and PC method.

3.1 IHS Method

The IHS method consists of four steps. (1) Three VGT bands are selected to represent the RGB color space. (2) A transformation in IHS space is applied. (3) The intensity component is substituted by the ASAR image. Before doing so, the ASAR image is first rescaled to match the standard deviation and the mean of the intensity image. (4) An inverse color transformation is performed, resulting in three fused bands.

3.2 PC Method

The PC method is very similar to the IHS method. (1) A number of VGT bands are selected. (2) A PC transformation is applied with the selected bands. (3) The first PC is replaced with the ASAR image. Again, the ASAR image is first rescaled to match the mean and standard deviation of the first PC. (4) An inverse PC transform is performed, resulting in three merged bands.

3.3 Wavelet-based methods

Let I_k be an image with spatial resolution k. A series of approximations A_j can be constructed using a dilated filter F_j:

$$\begin{aligned} A_1(I_k) &= F_1 I_k \\ A_2(I_k) &= F_2 A_1(I_k) \\ A_3(I_k) &= F_3 A_2(I_k) \\ &\cdots \end{aligned} \qquad \textbf{(1)}$$

At each decomposition level j spatial resolution is halved and equal to k (2^j). The filter F_j has a B_3 cubic spline profile [6]. The use of a B_3 cubic spline leads to a convolution with a 5 x 5 mask:

$$\frac{1}{256}\begin{pmatrix} 1 & 4 & 6 & 4 & 1 \\ 4 & 16 & 24 & 16 & 4 \\ 6 & 24 & 36 & 24 & 6 \\ 4 & 16 & 24 & 16 & 4 \\ 1 & 4 & 6 & 4 & 1 \end{pmatrix} \quad \textbf{(2)}$$

The dilatation of the filter is obtained by inserting ($2^j - 1$) zeros between the non-zero elements of F_j.
The detail image $D_j(I_k)$, containing all spatial structures with sizes between resolution levels j - 1 and j, is calculated as the difference between two consecutive approximation images:

$$D_j(I_k) = A_j(I_k) - A_{j-1}(I_k) \quad \textbf{(3)}$$

The original image I_k can be reconstructed by adding all detail images to the last approximation image.
Image fusion can be performed by combining the ASAR details and approximations with the different VGT bands. In this study, two approaches are followed: Method A and Method B.
Method A combines the spatial detail of the ASAR image with the spectral information of VGT and consists of the following steps. (1) A VGT band is selected and resampled (bilinear resampling) to match the pixel spacing of the ASAR image (75 m). (2) The ASAR image is rescaled to match the standard deviation of the VGT band. (3) The ASAR image is decomposed into four detail images ($D_{75\text{-}150}$, $D_{150\text{-}300}$, $D_{300\text{-}600}$ and $D_{600\text{-}1200}$) and one approximation image (A_{1200}). (4) A_{1200} is substituted by the resampled VGT band and an inverse wavelet transform is performed by adding the ASAR detail images to the VGT band.
Method B is based on the method proposed in [8]. In this method, the lower frequency components at lower scales are fused as well. The first three steps of Method B are the same as in Method A. Then, instead of substituting A_{1200} with the resampled VGT band, both images are multiplied. Next, the product is rescaled to match the standard deviation and mean of A_{1200}. Finally the ASAR detail images are added to the rescaled product.

4. EVALUATION OF FUSED IMAGES

The quality of the fused images was evaluated by visual inspection of a color composite image of the merged bands and by comparing classification results obtained by using a maximum likelihood classifier. For each method, the fused bands together with the original ASAR image were classified and the Kappa (κ) coefficient [12] was calculated. The Z-test for normal distributions was used to detect significant differences between classified image pairs for the kappa coefficients [13]:

$$Z = \frac{\kappa_2 - \kappa_1}{\sqrt{\sigma_{\kappa_1}^2 + \sigma_{\kappa_2}^2}} \quad \textbf{(4)}$$

5. RESULTS AND DISCUSSION

Four methods were used to fuse the ASAR image with the red, the NIR and the SWIR band of the VGT image. Each fusion resulted in three merged bands. Fig. 2 shows color composite images of the resulting merged bands for the different methods, together with the ASAR image and a color composite of the original VGT bands.

5.1 Visual inspection

Visual inspection revealed that Method A better preserves the spectral values of the original VGT bands, while spatial details induced by the ASAR image are still apparent (Fig. 2c). When the IHS and PC methods are used the spectral values of the original VGT bands are completely altered, as can be observed in Fig. 2e and Fig. 2f. This can be explained by the low correlation between the ASAR image and the image that is substituted (intensity component and PC1).

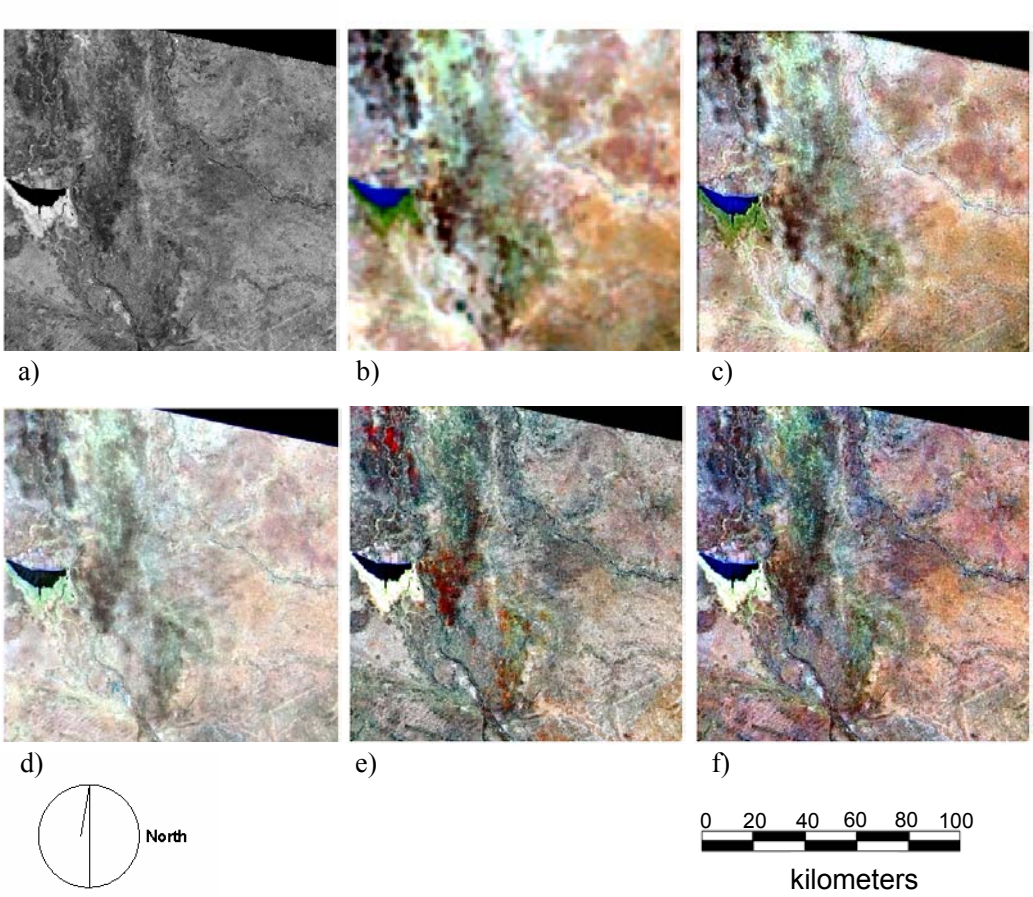

Fig. 2. Original images and color composite images of fused bands (B=red; G=NIR; R=SWIR) (a) ASAR image; (b) VGT image; (c) Method A; (d) Method B; (e) IHS method; (f) PC method

Intermediate results can be observed for Method B (Fig. 2d). When this method is used, the fused bands show higher correlations with the ASAR image, compared to the fused bands of method A. This is because the low frequency components of both data types are fused as well.

5.2 Classification results

For each fusion method a classification was performed, using the merged bands together with the ASAR image. For reasons of comparison, the original VGT bands together with the ASAR image, and both data sources separately were classified as well. Only the top left part of the images, containing the Logone floodplain, was classified. Seven land cover/ land use classes were considered: open water, three different wetland types and three different dry land types. Overall accuracy and kappa coefficients for the different methods are shown in Table 1.

Table 1 Overall accuracy (O.A.), Kappa coefficient (κ) and Kappa variance (σ_κ^2) of the classifications obtained using the different methods

Method	O.A. (%)	κ	σ_κ^2
Method B + ASAR	98	0.9750	0.000024
Method A + ASAR	97	0.9642	0.000029
VGT + ASAR	97	0.9592	0.000033
VGT	88	0.8708	0.000096
IHS + ASAR	87	0.8533	0.000107
PC method + ASAR	85	0.8275	0.000122
ASAR	68	0.6283	0.000211

All classifications, except for the classification of the ASAR image, show high levels of accuracy, since only well separable classes were considered. The wavelet-based fusion methods result in significantly higher kappa coefficients compared to the IHS and PC methods. When a classification is performed based on the original VGT bands and the ASAR image, a similar accuracy is obtained compared to the classification resulting from the fused bands obtained by Method A and Method B. However, with the wavelet-based fusion methods, the land cover/ land use classes are mapped with higher spatial detail. This can be observed in Fig. 3, showing the classification results and a subscene in detail.

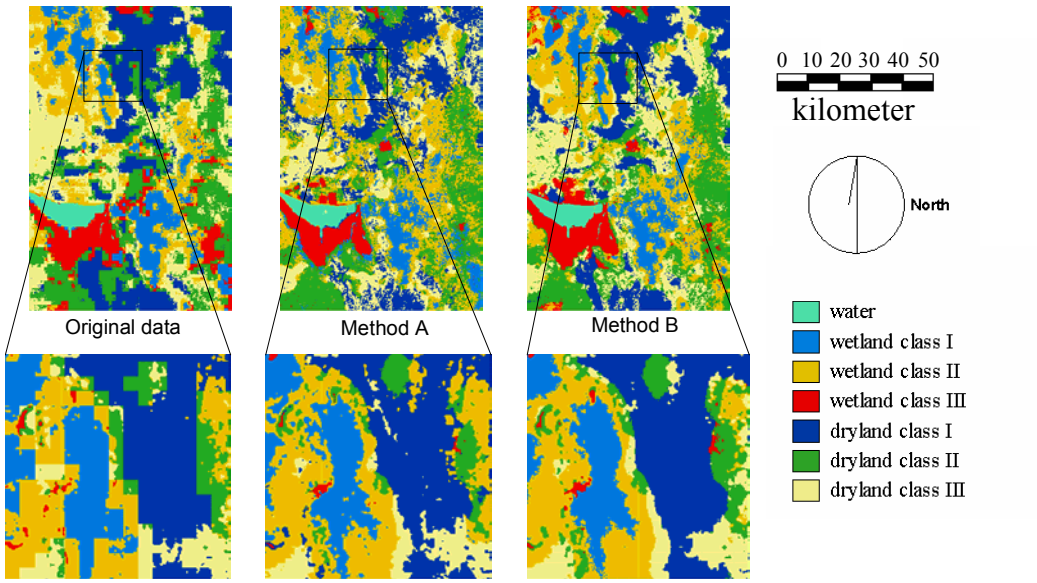

Fig. 3. Classification results with (a) original data; (b) Method A + ASAR; (c) Method B + ASAR

A negative effect of the wavelet-based fusion methods is that artefacts may appear, resulting in classification errors. This is especially the case for Method A. When Method B is used, this problem is minimized, due to the multiplication operation performed. This can be seen in Fig. 4, showing a subscene in detail, containing Water and Wetland. In the classification resulting from Method A, classification errors resulting from artefacts can be observed at the border between the two classes. This is not the case for Method B.

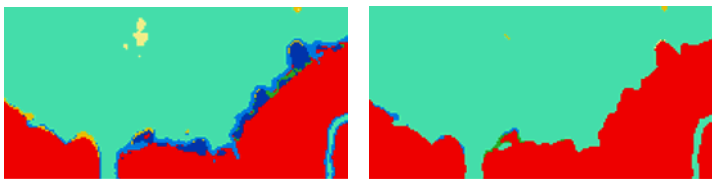

Fig. 4. Sub scene of classifications with Method A (left) and Method B (right)

5 CONCLUSIONS

Two wavelet-based fusion methods were used to combine ENVISAT/ ASAR Wide Swath and SPOT/VEGETATION D-10 data. The purpose of the data fusion was feature enhancement and improving classification accuracy of a tropical wetland located in the Lake Chad basin. The proposed methods outperformed the PC and IHS methods for both objectives. From all methods, Method A, best preserved the spectral values of the original VGT bands. The highest classification accuracies were obtained using the fusion results of Method B.

This work has shown that, in case of wetland mapping, wavelet fusion methods can be effective for the combination of ENVISAT ASAR Wide Swath data and SPOT-VEGETATION optical data, and can lead to improved classification results. Furthermore, since both image types have a high temporal resolution and cover large areas, the proposed fusion methods can be incorporated in wetland monitoring schemes.

6 ACKNOWLEDGMENTS

Funding of this project was provided by the Belgian Science Policy through a PRODEX contract (project No 15447). The ENVISAT ASAR data were made available by ESA in the framework of AO ID 467.

7 REFERENCES

1. Held A., et al. High resolution mapping of tropical mangrove ecosystems using hyperspectral and radar remote sensing, *International Journal of Remote Sensing*, Vol. 24, 2739-2759, 2003.
2. Kushwaha S.P.S., Dwivedi R.S. and Rao B.R.M. Evaluation of various digital image processing techniques for detection of coastal wetlands using ERS-1 SAR data, *International Journal of Remote Sensing*, Vol. 21, 565-579, 2000.
3. Pohl C. and Van Genderen J.L. Multisensor image fusion in remote sensing: concepts, methods and applications, *International Journal of Remote Sensing*, Vol. 19, 823-854, 1998.
4. Núñez J., et al. Multiresolution-Bases image fusion with Additive Wavelet Decomposition, *IEEE Transactions on Geoscience and Remote Sensing*, Vol. 37, 1204-1211, 1999.
5. Ranchin T. and Wald L. Fusion of High Spatial and Spectral Resolution Images: The ARSIS Concept and Its Implementation, *Photogrammetric Engineering & Remote Sensing*, Vol. 66, 49-61, 2000.
6. Aiazzi B. et al. Context-Driven Fusion of High Spatial and Spectral Resolution Images Based on Oversampled Multiresolution Analysis, *IEEE Transactions on Geoscience and Remote Sensing*, Vol. 40, 2300-2312, 2002.
7. Teggi S., Cecchi R. and Serafini F. TM and IRS-1C-PAN data fusion using multiresolution decomposition methods based on the 'a tròus' algorithm, *International Journal of Remote Sensing*, Vol. 24, 1287-1301, 2003.
8. Du Y.,Vachon P.W. and van der Sanden J.J. Satellite image fusion with multiscale analysis for marine applications: preserving spatial information and minimizing artifacts (PSIMA), *Canadian Journal of Remote Sensing*, Vol. 29, 14-23, 2003.
9. Ranchin T. and Wald L. The wavelet transform for the analysis of remotely sensed data, *International Journal of Remote Sensing*, Vol. 14, 615-619, 1993.
10. Mallat S.G. A Theory for Multiresolution Signal Decomposition: The Wavelet Representation, *IEEE Transactions on pattern analysis and machine intelligence*, Vol. 11, 674-693, 1989.
11. Starck J.L. and Murtagh F. Image restoration with noise suppression using the wavelet transform, *Astronomy and Astrophysics*, Vol. 288, 342-350, 1995.
12. Cohen J. A coefficient of agreement for nominal scale, *Educational and Psychological Measurement*, Vol. 20, 37-46, 1960.
13. Zar J. H. *Biostatistical analysis*, Prentice-Hall International, New Jersey, 1996.